The Hume-Rothery Electron Concentration Rules and Second Moment Scaling

Laura M. Hoistad and Stephen Lee*

Contribution from the Department of Chemistry, The University of Michigan, Ann Arbor, Michigan 48109. *Received October 25, 1990*

Abstract: We show that the Hume-Rothery electron concentration rules for noble-metal and transition-metal alloys can be understood through simple molecular orbital theory. We consider simple structure types such as the face-centered-cubic, hexagonal-closest-packed, and body-centered-cubic structures as well as more complex structure types such as the σ-phase, χ-phase, γ-brass, and β-Mn structures. Our results are the first theoretical calculations that corroborate the entire set of Hume-Rothery electron concentration rules.

Electron-counting rules have preoccupied chemists for most of this century. In molecular chemistry, the most famous examples of these rules are the octet and 18-electron rules for main-group and transition-metal compounds, the $4N + 2$ rule for ring systems, the VSEPR rules for AX_n molecules, and Wade's rule for electron-deficient clusters.[1] Many molecular chemists are, however, unaware that a parallel set of rules has also been developed for extended solids. Among the best known of these are the Grimm-Sommerfeld rule for main-group compounds and the Hume-Rothery rules for alloys.[2] The principal concern of this paper is the Hume-Rothery rules. These rules state that particular alloy crystal structure types are found at specific electron to atom ratios (e^-/a, i.e., the ratio of the number of valence electrons to the number of atoms). Structure types which are known to obey these electron concentration rules include the face-centered-cubic (fcc), hexagonal-closest-packed (hcp), body-centered-cubic (bcc), the β-Mn, the α-Mn (χ-phase), and the CrFe (σ-phase) structure types, for both transition-metal and noble-metal alloys.[3]

The theoretical basis for the Hume-Rothery rules has been extensively investigated. Earlier researchers favored explanations based on the free electron model.[4] More modern workers have found that pseudopotential methods give more reliable answers.[5] However, the pseudopotential methods have only been used to investigate the simpler structure types such as fcc, hcp, and bcc.[6] To date, no one has investigated the more complicated phases such as γ-brass (52-atom cubic unit cell), β-Mn (20-atom cubic unit cell), χ-phase (58-atom cubic cell), or σ-phase (30-atom tetragonal cell). As these complex phases form a fair fraction of the phases for which there are known electron to atom ratios (e^-/atom), this pseudopotential work is incomplete. Thus, over 60 years after Hume-Rothery's initial formulation of his rules, theorists are still unable to say that they have developed a theory which accounts for the entire set of rules. Futhermore, the theoretical work which has been done is perplexingly different from the theory which has developed for molecular electron counting rules. For example, pseudopotential calculations on the stability of fcc, bcc, and hcp as a function of electron count have led researchers to conclude that the Hume-Rothery rules are due to "rapid variation of the polarizability in the vicinity of $2k_F$."[6a] Such a statement is based on ideas which are completely different from the rather simple molecular orbital ideas which form the basis of our understanding of Wade's rules, VSEPR, and the Hückel $4N + 2$ rule.

In this article we show that a simple molecular orbital theory can indeed account for *all* the Hume-Rothery electron concentration rules for both noble-metal and transition-metal alloys. The theoretical basis of our work is identical with the commonly accepted theoretical basis for molecular electron-counting rules and does not require complex physical concepts. Furthermore, our results are the first complete set of calculations over the full range of Hume-Rothery phases.

Second Moment Scaling. The aforementioned electron-counting rules for molecules can be rationalized through the judicious use of Hückel or extended Hückel molecular orbital theory. One cannot, however, fruitfully apply these Hamiltonians to directly calculate the total electronic energies of the different noble metal alloy structure types. To understand why this is so, it is useful to consider a much simpler chemical system. In particular we consider the H_2 molecule. In Hückel theory one finds that H_2 has a bonding molecular orbital with energy β and an antibonding molecular orbital with energy $-\beta$. The energy β is generally taken to be proportional to the overlap integral of the two hydrogen 1s atomic orbitals. This overlap integral increases as the distance between the two hydrogens decreases. Therefore, as the interatomic distance of the H_2 molecule decreases, the total energy in a Hückel calculation also decreases. It is this correlation between bond lengths and electronic energy which is the source of much of the energetic inaccuracies in Hückel theory. For example, in the case of the H_2 system the interatomic distance which minimizes the total Hückel electronic energy is zero. Hückel theory predicts the most stable form of H_2 is He.

To correct for this error, one must include electron-electron repulsion energies. Unfortunately, it is difficult to devise a procedure which both accurately calculates this repulsive energy and also keeps the comparatively simple form is Hückel theory. However, recent studies of intermetallic crystal phases[7] have shown it is possible to devise a simple ad hoc method which obviates the need to directly calculate electron-electron repulsion energies. We

* Author to whom correspondence should be addressed.

(1) (a) Yates, K. *Hückel Molecular Orbital Theory*; Academic Press: New York, 1978. (b) Heilbonner, E.; Bock, H. *The HMO-Model and its Applications*; Wiley: New York, 1976. (c) Albright, T. A.; Burdett, J. K.; Whangbo, M. H. *Orbital Interactions in Chemistry*; Wiley: New York, 1985. (d) Wade, K. *Adv. Inorg. Chem. Radiochem.* **1976**, *18*, 1.

(2) (a) Hume-Rothery, W.; Raynor, G. V. *The Structure of Metals and Alloys*; Institute of Metal: London, 1962. (b) Hume-Rothery, W. In *Phase Stability in Metals and Alloys*; Rudman, P. S., Stringer, J., Jaffee, R. I., Eds.; McGraw-Hill: New York, 1976; p 3. (c) For a discussion of the Grimm-Sommerfeld rule, see: Burdett, J. K. *Molecular Shapes*; Wiley: New York, 1980; p 269.

(3) (a) β-Mn($SiCu_5$): Arrhenius, S.; Westgren, A. *Z. Phys. Chem. Abt. B* **1931**, *14*, 66. (b) α-Mn (χ-phase): Bradley, A. J.; Thewlis, J. *Proc. R. Soc. London, A* **1927**, *115*, 456. (c) CrFe (α-phase): Dickins, G. J.; Douglas, A. M. B.; Taylor, W. H. *Acta Crystallogr.* **1956**, *9*, 297.

(4) Mott, N. F.; Jones, J. *The Theory of the Properties of Metals and Alloys*; Oxford University Press: Oxford, 1936.

(5) (a) Heine, V.; Weaire, D. *Solid State Phys.* **1970**, *24*, 247. (b) Yin, M. T.; Cohen, M. L. *Phys. Rev. Lett.* **1980**, *45*, 1004. (c) Yin, M. T.; Cohen, M. L. *Phys. Rev. B: Condens. Matter* **1981**, *24*, 6121; **1982**, *26*, 5668.

(6) (a) Stroud, D.; Ashcroft, N. W. *J. Phys. F: Met. Phys.* **1971**, *1*, 113. (b) Evans, R.; Lloyd, P.; Mujibur Rahman, S. M. *J. Phys. F: Met. Phys.* **1979**, *9*, 1939. (c) Borisova, S. D.; Zhorovkov, M. F.; Paskal, Y. I. *Sov. Phys. Solid State (Engl. Transl.)* **1985**, *27*, 400. (d) Mujibur-Rahman, S. M. *J. Phys. F: Met. Phys.* **1981**, *11*, 1191. (e) Krause, C. W.; Morris, J. W., Jr. *Acta Metall.* **1974**, *22*, 767. (f) Cousins, C. S. G. *J. Phys. F: Met. Phys.* **1974**, *4*, 1.

(7) Early applications of the second moment scaling hypothesis are (a) for AB (main group and transition metal) phases in Pettifor, D. G.; Podloucky, R. *Phys. Rev. Lett.* **1984**, *53*, 1080, and (b) for the Peierls distortion in Burdett, J. K.; Lee, S. *J. Am. Chem. Soc.* **1985**, *107*, 3063. More recent work includes: (c) Cressoni, J. C.; Pettifor, D. G. *J. Phys. Condens. Matter* (submitted for publication), (d) Lee, S. *J. Am. Chem. Soc.* **1991**, *113*, 101, and (e) for elemental structures: Lee, S. *J. Am. Chem. Soc.* (submitted for publication).

0002-7863/91/1513-8216$02.50/0

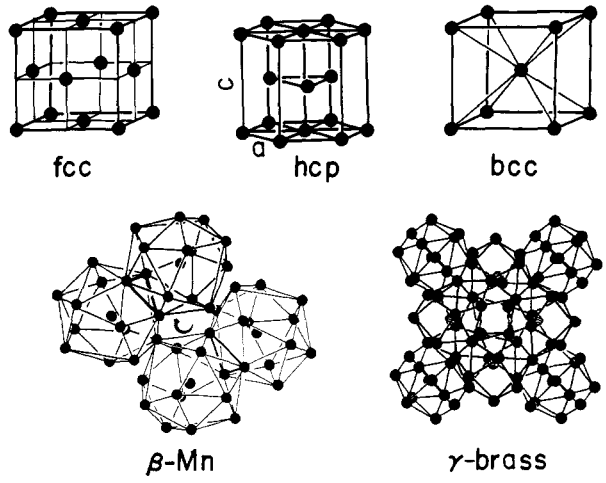

Figure 1. The fcc, hcp, bcc, β-Mn and γ-brass structure types.[3,11] The β-Mn and γ-brass structures are reasonably complicated. The β-Mn structure can be considered to be composed of 14-coordinate polyhedra which are face and vertex sharing. These form spirals (see arrow in drawing). Surrounding the illustrated spirals are four more spirals which twist in the opposite direction. The γ-brass structure is composed of 13-coordinate polyhedra. In our drawing we show four of these polyhedra (in the center of the drawing) surrounded by another four at the corners of the drawing. In the β-Mn and γ-brass drawings, all lines represent bonds. All bonds are drawn except those which involve atoms at the center of each polyhedron. Finally, in the hcp drawing we indicate the c and a distances which form the basis of the c/a ratio used to classify hcp structures. At $c/a = 1.633$, each atom has 12 nearest neighbors. As one deviates from this value, each atom has six first-nearest neighbors and six second-nearest neighbors.

call this method second moment scaling. This second moment scaling hypothesis was first proposed a number of years ago by several authors.[7] Pettifor and Podloucky showed that with second moment scaling they were able to explain the qualitative trends that occurred for AB compounds where A was a transition element and B a main-group element. Burdett and Lee showed that second moment scaling was necessary if one were to correctly model the Peierls distortion. The Pettifor and Podloucky work is particularly interesting as it offers an explanation as to why second moment scaling is effective.

The method relies on setting the variance of molecular orbital energies to a fixed value. The variance follows the formula, variance $= (1/n)\sum_{i=1}^{n}(E_i - E_{av})^2$, where n is the number of molecular orbitals, E_i is the energy of the ith molecular orbital, and E_{av} is the average energy of the molecular orbitals. For example, from the perspective of this method, the difficulty we encountered in our analysis of H_2 was that we did not keep variance fixed. Were we to have fixed variance to a reasonable value, the distance between hydrogen atoms would have been fixed as decreasing this distance would change the overall variance.

We can use second moment scaling when we compare the energies of structure types with different coordination numbers. Without modification, Hückel theory would generally predict that the geometry with the largest coordination number would be lower in energy. This is because in such a structure the average overlap integral will be larger. In order to compensate for this error we fix each structure type to have the same variance. In practice we change the overall density of the various crystals until the variances of their molecular orbital energies are exactly equal. Other than this, we use a standard Hückel method in our band calculations. The diagonal elements of our Hückel–Hamiltonian are taken from the set of parameters developed by R. Hoffmann and others.[8] We use the Wolfsberg–Helmholz approximation[9] in calculating off-diagonal elements. Unlike extended Hückel[10] calculations, we solve the secular equation $H\psi = E\psi$ and not $H\psi = ES\psi$.

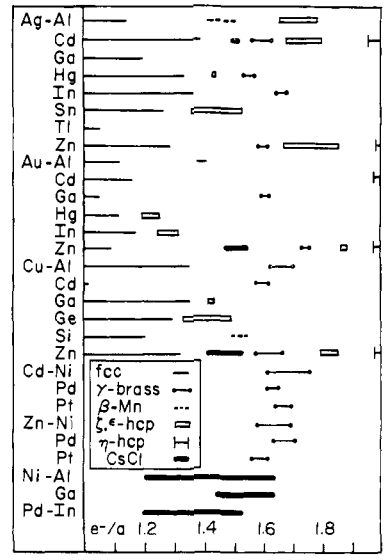

Figure 2. Known low-temperature examples of binary Hume–Rothery noble and main group metal alloys classified by electron concentration (e^-/a). Data taken from ref 13.

Noble-Metal Alloys. Five phases form the basis of the Hume–Rothery electron-counting rules for noble-metal alloys. They are hcp, bcc, fcc, β-Mn, and the γ-brass structure types.[11,12] These last two structures are quite complicated and are illustrated together with the three simpler structures in Figure 1. The hcp structure type is subject to a wide variation in its c/a ratio and is often divided into three different branches. For ζ-hcp, the c/a ratio (see Figure 1) is near the ideal value of 1.633. The ϵ-hcp form has a contracted c/a value which ranges from 1.58 to 1.55 while for η-hcp the c/a value ranges from 1.77 to 1.88. It should be noted that these different hcp types can be genuinely different. For example, in the Ag–Zn, Au–Zn, Cu–Zn and Ag–Cd binary-phase diagrams there are biphased regions where both phases are hcp—one phase being η and the other ϵ!

In Figure 2 we compile the known examples of Hume–Rothery binary alloys.[13] In this figure we restrict ourselves to the low-temperature regime of the phase diagram (as our model corresponds to a zero Kelvin calculation). It may be seen that at the lowest temperatures shown on the binary-phase diagrams there are no known disordered bcc alloys. All bcc materials order at low temperature either to a bcc superstructure or to another entirely different structure type. We indicate in Figure 2 the CsCl structure, which is the most common ordered form of the bcc structure. We summarize the data for the observed electron counts in Table I.

We plot in Figure 3a the difference in structural energy as a function of band filling on the basis of Hückel calculations. In Figure 3a we consider an s and p band model. We see at slightly

(8) (a) A compilation of eH parameters mainly established by the R. Hoffmann group at Cornell has been collected by S. Alvarez (University of Barcelona, 1987). This compilation is unpublished. (b) For this paper we use main group atom parameters from Thorn, D. L.; Hoffmann, R. *Inorg. Chem.* **1978**, *17*, 126 and (c) Fe parameters from Summerville, R. H.; Hoffmann, R. *J. Am. Chem. Soc.* **1976**, *98*, 7240.

(9) Wolfsberg, M.; Helmholz, L. *J. Chem. Phys.* **1952**, *20*, 837.

(10) (a) Hoffmann, R. *J. Chem. Phys.* **1963**, *39*, 1397. (b) Hoffmann, R.; Lipscomb, W. N. *J. Chem. Phys.* **1962**, *36*, 2179. (c) Whangbo, M-H.; Hoffmann, R.; Woodward, R. B. *Proc. R. Soc. London, A* **1979**, *366*, 23.

(11) γ brass (Cu_5Zn_8): Heidenstam, O. V.; Johansson, A.; Westman, S. *Acta Chem. Scand.* **1968**, *22*, 653.

(12) See discussion by Massalski, T. B. In *Physical Metallurgy*, 3rd ed.; Cahn, R. W.; Haasen, P., Eds.; North Holland Physics: Amsterdam, 1983; p 153.

(13) (a) Villars, P.; Calvert, L. D. *Pearson's Handbook of Crystallographic Data for Intermetallic Phases*; American Society for Metals: Metal Park, OH, 1985. (b) Hansen, M. *Constitution of Binary Alloys*; McGraw-Hill, New York, 1958. (c) Elliott, R. P. *Constitution of Binary Alloys* (First Supplement); McGraw-Hill: New York, 1965. (d) Shunk, F. A. *Constitution of Binary Alloys* (Second Supplement); McGraw-Hill: New York, 1969. (e) Moffat, W. G. *The Handbook of Binary Phase Diagrams* (Genium A); Schnectady, New York, 1987.

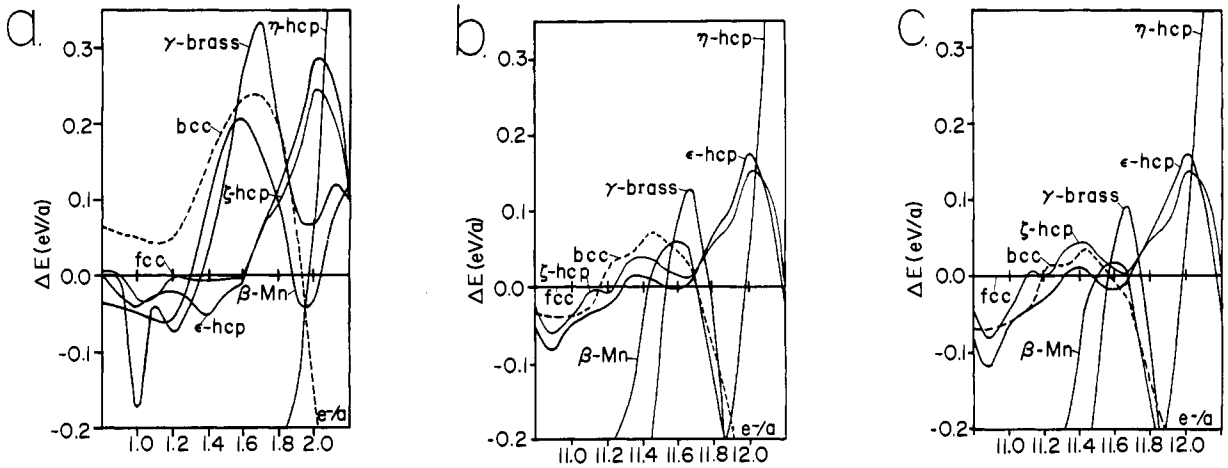

Figure 3. The difference in electronic energy per atom between the fcc, bcc, ζ-hcp, ϵ-hcp, η-hcp β-Mn, and γ-brass structure types as a function of the number of valence electrons per atom (e^-/a). Throughout this figure the following convention is used. We plot the difference in energy between any structure type and the fcc structure. Thus in Figure 3a, the ζ-hcp structure is more stable than the fcc structure for 1.95 e^-/a and higher e^-/a values, while fcc is more stable than ζ-hcp below 1.95 e^-/a. We can therefore quickly determine at any particular electron count which structure type is the most stable. For example, in Figure 3a the γ-brass curve is the most positive curve between 1.55 and 1.80 e^-/a. Therefore, γ-brass is the most stable structure type at these electron counts. In all three parts of this figure the bcc curve (for the sake of clarity) is drawn as a dotted line. In all the calculations, we have scaled the atomic density to give a second moment equal to that calculated for the Cu_5Si (β-Mn) crystal structure. The compound used in the γ-brass calculations was the crystal structure of Cu_5Zn_8. For ζ-hcp we set $c/a = 1.633$, for η-hcp $c/a = 1.85$, and for ϵ-hcp $c/a = 1.58$. There are no adjustable parameters for the bcc and fcc structure types. Finally, in Figure 3a we used the parameters we used in a previous paper.[8b,14] Only one atom type (with 4s and 4p valence orbitals) was considered: H_{ii} (4s) = −16.0 eV, H_{ii} (4p) = −9.0 eV; ζ(4s) = 2.16, ζ(4p) = 1.85. Slater type orbitals were used. In (b) a 3d orbital component was also added: H_{ii}(3d) = −60.0 eV, ζ(3d) = 3.0. (A single ζ expansion was used.) In (c) ζ(3d) = 2.9 and H_{ii}(3d) = −60.0 eV. The k-point meshes were taken over the irreducible wedge k space. The fcc and bcc calculation used a 165-point simple cubic mesh. All hcp forms used a 147 hexagonal k-point mesh. β-Mn used a 10 k-point-simple cubic mesh and γ-brass used a 8 k-point body-centered mesh.

Table I. Noble Electron Phases Found between 1 and 2 s and p e^-/a

	experimentally found range		predicted range		
phase	all temp	low temp	s and p model[a] (w/o bcc)	s, p, and d model with ζ(3d) = 2.9[a,b]	s, p, and d model with ζ(3d) = 3.0[a,b]
fcc	1.00–1.35	1.00–1.40	1.00–1.31	11.00–11.20	11.00–11.28
ζ-hcp	1.22–1.75	1.22–1.55	1.14–1.31	11.07–11.39	11.09–11.58
				11.73–11.87	11.73–11.87
bcc	1.36–1.59	1.20–1.65[c]		11.12–11.58	11.16–11.56
β-Mn	1.40–1.54	1.40–1.54	1.28–1.56	11.51–11.60	11.50–11.60
γ-brass	1.54–1.70	1.55–1.75	1.52–1.85	11.56–11.75	11.56–11.73
ϵ-hcp	1.66–1.89	1.66–1.89	1.82–2.06	11.73–12.03	11.71–12.03
η-hcp	1.96–2.00	1.97–2.00	>2.06	>12.03	>12.03

[a] Structure type within 0.02 eV/atom of the most stable structure type. [b] The addition of the d orbital contributes 10 more e^-/atom. [c] The bcc range is based on the low-temperature CsCl phases (CsCl is an ordered bcc structure type).

above 2 e^-/a that η-hcp is the most stable structure, while ϵ-hcp is the most stable one from 1.85 to 2.05 e^-/a and finally that γ-brass is the most stable structure from 1.55 to 1.85 e^-/a. This correlates quite well with the experimental results compiled in Figure 2 and Table I. At lower electron counts, however, the results of Figure 3a indicate the bcc structure is more stable for all electron counts. This is not in agreement with experiment. Ignoring the incorrect bcc curve for now, we see that β-Mn is stable from 1.30 to 1.55 e^-/a, both fcc and ζ-hcp are stable from 1.20 to 1.30 e^-/a, and fcc alone is almost stable from 1.00 to 1.20 e^-/a. However, below 0.9 e^-/a, both ζ-hcp and ϵ-hcp have energies near that of fcc. These results are tabulated in the third column of Table I. It may be seen that if the bcc curve is excluded, then aggrement between theory and experiment is reasonable. However, all our results are under the shadow of the spurious bcc curve which dominates at low electron counts.

In considering the results based on a pure s and p model, it should be recalled that the noble metals straddle two different regimes of the periodic table. The elements to the right of them in the periodic table are main group atoms which truly have only s and p valence electrons. The elements to the left of them are transition elements where the valence electrons are primarily of s and d character. It may be seen that our s and p model should therefore provide a more reliable picture of the bonding closer toward 2 e^-/a, which is indeed the case. It is straightforward to show that the principal errors in Figure 3a are due to the absence of the d manifold of orbitals. In Figure 3b,c we present the results of our band calculations where a contracted d orbital has been included. There are two parameters which must be chosen in order for us to include a contracted d orbital. They are the H_{ii} Coulombic value and ζ, the Slater type orbital exponent size parameter. For systems with over 11 e^-/a (we include here the 10 d electrons in our electron counting) the d band is essentially filled. We therefore place the H_{ii} value at very low energy in order to insure complete filling of the d band. We are then left with ζ as the one adjustable parameter. We have chosen our ζ value in order to create the best possible fit between our theory and experiment. This is reasonable for two reasons. First, Hückel theory is said to be semiempirical. As Hückel theory works best at explaining structure, it is not unreasonable to use structural data as the empirical basis of the method. As second moment scaling is a rather new method; there is not a body of parameters which have been developed previously in the literature. In general, we use the parameters developed for the eH method. However, we have discovered previously that some modification of those parameters are necessary when dealing with contracted orbitals.[14] Second,

(14) Lee, S. *J. Am. Chem. Soc.* **1990**, submitted for publication. In this earlier work we showed that extensive contraction of the s orbital is necessary to model the inert pair effect in the main-group elements.

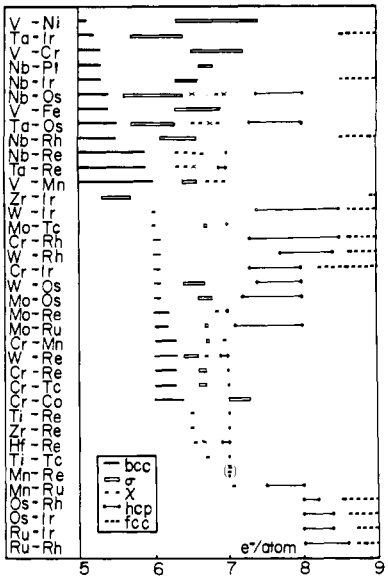

Figure 4. Known low-temperature examples of binary transition-metal fcc, bcc, hcp, χ- and σ-phase alloys classified by electron concentration (e^-/atom). Data taken from ref 13.

we are fitting seven different structure types (fcc, bcc, ζ-hcp, ϵ-hcp, η-hcp, β-Mn, and γ-brass) with only one adjustable parameter. Each structure type produces an entire loci (the curves shown in Figure 3) of predictions. The amount of information produced is therefore far in excess to the number of adjustable parameters.

The H_{ii} Coulombic value and the ζ exponent parameters which we have used in our calculations are quite different from the standard d-orbital parameters used in late transition metal extended Hückel calculations.[8] This difference stems from our use of Hückel rather than extended Hückel band calculations. Hückel calculations overestimate the bonding energy of the most bonding band orbitals. For this reason, if we wish to treat the d band as an occupied low-lying energy band we must place the d orbital at unnaturally low values. This choice of an H_{ii} value for the d orbitals also impacts the ζ exponent for these orbitals. This is so as we use in our calculations the Wolfsberg–Helmholz approximation for the off-diagonal terms in the Hamiltonian, H_{ij}. In this approximation $H_{ij} = KS_{ij}(H_{ii} + H_{jj})$. S_{ij} is the overlap integral, K is a proportionality constant, and H_{ii} and H_{jj} are Coulombic integral values. It is clear that if we overestimate the size of H_{ii} we must also underestimate the size of S_{ij} in order to maintain a correct overall H_{ij} value. In Hückel theory we are forced to set the Slater exponents to a large value so as to reduce the overall size of the overlap integrals.

With the inclusion of a contracted d orbital the agreement between theory and experiment becomes excellent. We compare the results of our theory and experiment in Table I. It should be noted that one must now add 10 electrons to the experimental results as we now have included the d electrons. It may be seen that our calculations predict the correct boundary lines for each structure type to within 0.1 e^-/a of the experimentally determined lines. Thus, all the major features of the Hume–Rothery rules can be seen in our calculational results. In the Hume–Rothery rules at low e^-/a, first the fcc structure is most stable. As e^-/a is increased, ζ-hcp becomes a viable alternate, followed next by bcc, β-Mn, γ-brass, ϵ-hcp, and finally toward the limit of 2 e^-/a η-hcp. Our calculations place these structures in the same order. An equally strong point of our calculations is that they are able to account for the overlapping of the fcc, ζ-hcp, and bcc forms observed at the low e^-/a range. This is so because at these lower e^-/a values these three curves often lie within 0.02 eV/a of each other. Specific features of any given alloy (for example that the alloy is a Ag–Sn alloy vs a Ag–Al alloy) will certainly be responsible for individual variations of 1/2 kcal/atom!

Finally, it should be noticed that we have not included in our calculations potentially important energetic effects such as atomic size effects, order–disorder phenomena, and electronegativity differences between the constituent atoms. However, this is very much in keeping with the original Hume–Rothery electron concentration rules, which are based on the premise that it is electron concentration which is most significant in determining alloy crystal structure type for these phases.

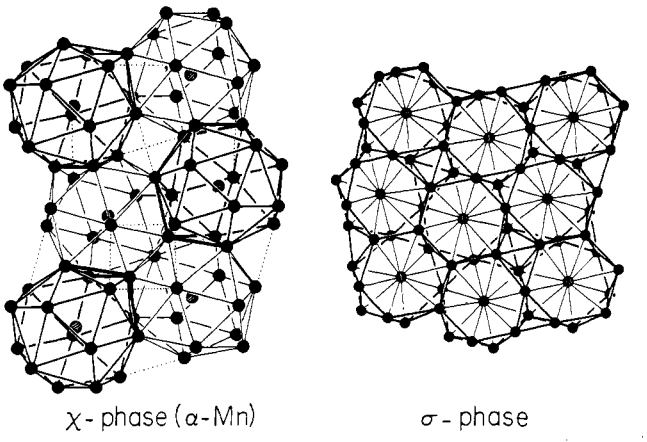

Figure 5. The χ- and σ-phases.

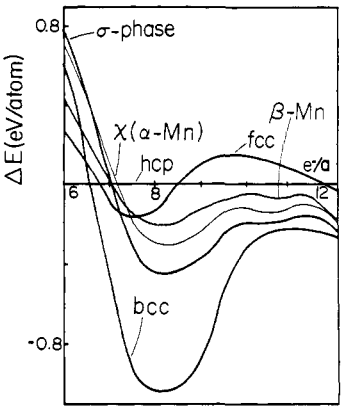

Figure 6. The difference in electronic energy per atom between the χ-phase (α-Mn), σ-phase, fcc, bcc, hcp, and β-Mn as a function of the number valence electrons per atom. Differences in energy between a given structure and the hcp structure are plotted. See the caption for Figure 3 for figure conventions. All atomic densities are adjusted to give the same second moment as found experimentally for the FeCr (σ-phase) alloy. Only one atom type was used. These were parameters previously used for Fe.[8c] $H_{ii}(4s) = -9.10$ eV, $H_{ii}(4p) = -5.32$ eV, $H_{ii}(3d) = -12.60$ eV; $\zeta(4s) = \zeta(4p) = 1.9$, $\zeta_1(3d) = 5.35$ (0.5505), $\zeta_2(3d) = 2.00$ (0.6260).

Transition-Metal Alloys. We now turn to the transition elements. One can construct a set of rules for transition-metal alloys which are analogous to the Hume–Rothery rules.[2b] In Figure 4 we show the thermodynamic stable phases for several binary alloy systems. The five phases shown are hcp, fcc, bcc, χ-phase (α-Mn) and σ-phase. These last two phases are illustrated in Figure 5. One tendency is to discount the χ-phase (α-Mn structure type) because α-Mn itself is antiferromagnetic. However, although Mn is the only element to be found in the α-Mn structure, there exist numerous other binary phases which are not antiferromagnetic which also adopt this structure (e.g., Ta–Os, Nb–Os, Ta–Re, and Nb–Re alloys). Furthermore, these binary phases adopt the α-Mn structure at or near 7 e^-/a, the electron count of Mn itself. Therefore, in a study of transition-metal alloy structures, the α-Mn structure should be included. These five phases are all known to have specific allowed e^-/a values. These are shown in Table II. The hcp, fcc, and bcc phases have been previously studied by D. Pettifor.[15] However, in this earlier work the s and p bands were not included. As we showed earlier s, p, and d hybridization

(15) (a) Pettifor, D. G. *J. Phys. C: Solid State Phys.* **1970**, *3*, 367. (b) Pettifor, D. G. *Metall. Chem. Proc. Symp.*; Kubaschewski, O., Ed.; HMSO: London, 1972; p 191.

Table II. Transition-Metal-Alloy Electron Phases Found between 6 and 11 e^-/a[a]

phase	experimentally determined e^-/a	prediction based on s, p, and d model[b,c]
bcc	6.0–6.4	
σ-phase	6.0–7.3	6.0–7.0
χ-phase (α-Mn)	6.3–7.0	6.1–7.3
hcp	7.0–8.6	7.0–8.7
fcc	8.2–11.0	8.3–11.0

[a] Data are taken from the low-temperature region of the respective binary-phase diagrams. [b] Near 6.0 e^-/a, an s, d model with a more excited state p band becomes increasingly appropriate. See text for discussion of this point. [c] Values reported indicate that the reported structure type is within 0.05 eV/a of the most stable structure type's energy at a given electron count.

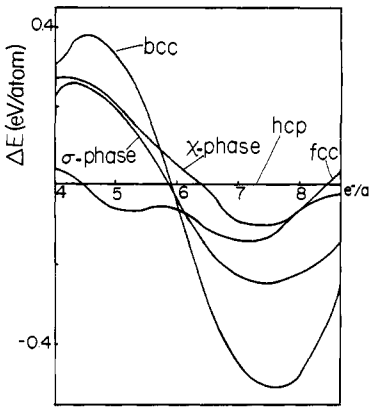

Figure 7. The difference in electronic energy per atom between the χ-phase (α-Mn), σ-phase, fcc, bcc, and hcp as a function of the number of valence electrons per atom. See the captions for Figures 3 and 6 for the figure conventions. The same Hückel parameters were used in this calculation except only 4s and 3d orbitals were used. All structures were scaled to the same second moment as that found experimentally for the FeCr (σ-phase) alloy.

plays an important role in the energetics of various structure types. We show the results of our calculations in Figure 6. It may be seen that agreement between our theory and experiment is excellent. Our calculations show that fcc is the most stable structure from 8.5 to 11.7 e^-/a. This is a significant improvement of the d orbital only model[15] which places bcc as the most stable structure at 10d e^-/a. Hcp is the most stable form in our calculations from 7.1 to 8.4 e^-/a, and the σ and χ phases are the most stable ones from 6.0 to 7.1 e^-/a. These results are in excellent agreement with experiment. Near 6 e^-/a, however, our model begins to break down. The reason for this breakdown is clear. As one turns to lower and lower e^-/a values, the p orbitals are becoming increasingly purely excited state orbitals. They therefore exert less stereochemical control. This is similar to the problem of the contracted d orbital in the noble-metal alloys. One important distinction must be made. In the case of a contracted orbital, it is straightforward within the confines of the Hückel model to model the effect of the contraction by increasing the ζ exponent parameters. Such an increase decreases the overall effect of the given orbital. However, in excited (diffuse) state orbitals, the ζ exponent decreases. Unfortunately, such a decrease in exponent value imparts a greater stereochemical weight to the diffuse orbital. It is therefore difficult to directly model the stereochemical effect induced by the p orbitals as it leaves the valence band and enters the excited bands. We can, however, obtain a qualitative picture of what happens when the p orbitals leave the valence band by eliminating the p orbitals altogether. We do so in Figure 7. It may be seen that in the absence of the p orbital, bcc becomes more favored over χ and σ from 5 e^-/a to near 6 e^-/a. This is in good agreement with the experimental results reported in Table II. The situation below 4 e^-/a however remains unresolved.

One point of interest is to examine qualitatively the effect of temperature on alloy crystal structure. Our results correspond to the crystal structures at absolute zero. As one leaves absolute zero, vibrational effects become increasingly important. An example of this may be seen in the elemental Mn structure. Solid Mn occurs in four different modifications, α-Mn (χ-phase), β-Mn, fcc, and bcc. These forms are the stable forms for four different temperature ranges. α-Mn is stable up to 729 °C, β-Mn is stable from 729 °C to 1095 °C, fcc is stable from 1095 °C to 1135 °C, and bcc is stable above 1135 °C. If one examines Figure 6, one sees that at 7e^-/a α-Mn is the most stable form, β-Mn is slightly less stable, fcc is even less stable, and bcc is the least stable of all the calculated possibilities. Thus, as temperature increases, the electronic factors play an ever decreasing role in predicting structure.

Acknowledgment. We thank the donors of the Petroleum Research Fund, administered by the American Chemical Society, and the Rackham Graduate School for support of this research. The band program used in our calculations is a modified version of the program written at Cornell University by Roald Hoffmann, M-H. Whangbo, T. Hughbanks, S. Wijeyesekera, M. Kertesz, C. N. Wilker, and C. Zheng. We also thank Gordon Miller for his irreducible wedge k-space programs.